IOP Conf. Series: Materials Science and Engineering **257** (2017) 012007 doi:10.1088/1757-899X/257/1/012007

Efficient operation scheduling for adsorption chillers using predictive optimization-based control methods

Adrian Bürger[1,3], Parantapa Sawant[2], Markus Bohlayer[1], Angelika Altmann-Dieses[1], Marco Braun[1] and Moritz Diehl[3]

[1] Faculty of Management Science and Engineering, Karlsruhe University of Applied Sciences, Moltkestraße 30, 76133 Karlsruhe, Germany
[2] Institute of Energy Systems Technology, Offenburg University of Applied Sciences, Badstraße 24, 77652 Offenburg, Germany
[3] Systems Control and Optimization Laboratory, Department of Microsystems Engineering, University of Freiburg, Georges-Koehler-Allee 102, 79110 Freiburg, Germany

E-mail: adrian.buerger@hs-karlsruhe.de

Abstract. Within this work, the benefits of using predictive control methods for the operation of Adsorption Cooling Machines (ACMs) are shown on a simulation study. Since the internal control decisions of series-manufactured ACMs often cannot be influenced, the work focuses on optimized scheduling of an ACM considering its internal functioning as well as forecasts for load and driving energy occurrence. For illustration, an assumed solar thermal climate system is introduced and a system model suitable for use within gradient-based optimization methods is developed. The results of a system simulation using a conventional scheme for ACM scheduling are compared to the results of a predictive, optimization-based scheduling approach for the same exemplary scenario of load and driving energy occurrence. The benefits of the latter approach are shown and future actions for application of these methods for system control are addressed.

1. Introduction

Adsorption Cooling Machines (ACMs) provide possibilities for more ecological cooling energy production [1]. Therefor, multiple control aspects have been examined in the literature to increase the operation efficiency of ACMs, e. g. by (predictive) optimization of cycle times [2, 3] or by reducing the electrical energy consumption by situational control of pump and recooling tower fan speeds [4]. While series-manufactured machines typically are equipped with internal controllers whose strategies are determined by the manufacturer and cannot be altered or influenced externally, and/or are missing additional measurement devices (e. g. internal pressure sensors [2]) that allow for more elaborate control strategies, an aspect that can be optimized without changing a machine's internal control logic is to predictively schedule its operation times in a way to enable efficient operation, considering its internal functioning and control decisions.

The current temperatures of the mass flows entering an ACM are crucial for its operation efficiency [1]. Attractive providers of driving energy for ACMs are low-temperature waste heat of industrial processes or solar thermal power [5]. In both cases, the availability of driving energy is predictable in the form e. g. of production plans or weather forecasts, respectively. This favors the use of optimization-based predictive control methods, where in contrast to conventional set-point based controllers, predictions can be taken into account directly to determine at which

times machine operation needs to be scheduled to be efficient, and how operating the ACM itself will affect these operation conditions. Such considerations can increase the operation efficiency, and with this, also reduce the operation time that is needed to provide a certain cooling demand.

Since predictive control methods are well-suited for control of systems with slow system response, such methods have been shown to be advantageous for control of Heating, Ventilation and Air Conditioning (HVAC) systems of buildings [6], which favors an inclusion of ACM scheduling. Further improvements to internal machine control strategies can be incorporated independently. However, compared to conventional controllers, these control methods need more information on the considered system in the form e. g. of suitable system models and forecasts.

Within this work, the benefits of using predictive control methods for operation scheduling of a silica-gel/water ACM are shown on a simulation study for a solar thermal HVAC system. First, the assumed system and the chosen modeling approach are described. Then, the model is simulated for a test scenario using a conventional control scheme. Afterwards, an optimization-based controller is applied to the system for the same test scenario, and the performance of both controllers is compared. The benefits of the optimization-based approach are shown, and future actions for application of these methods for system control are addressed.

2. Experimental setup

Within this simulation study, a solar thermal HVAC system as shown in Figure 1 is considered.

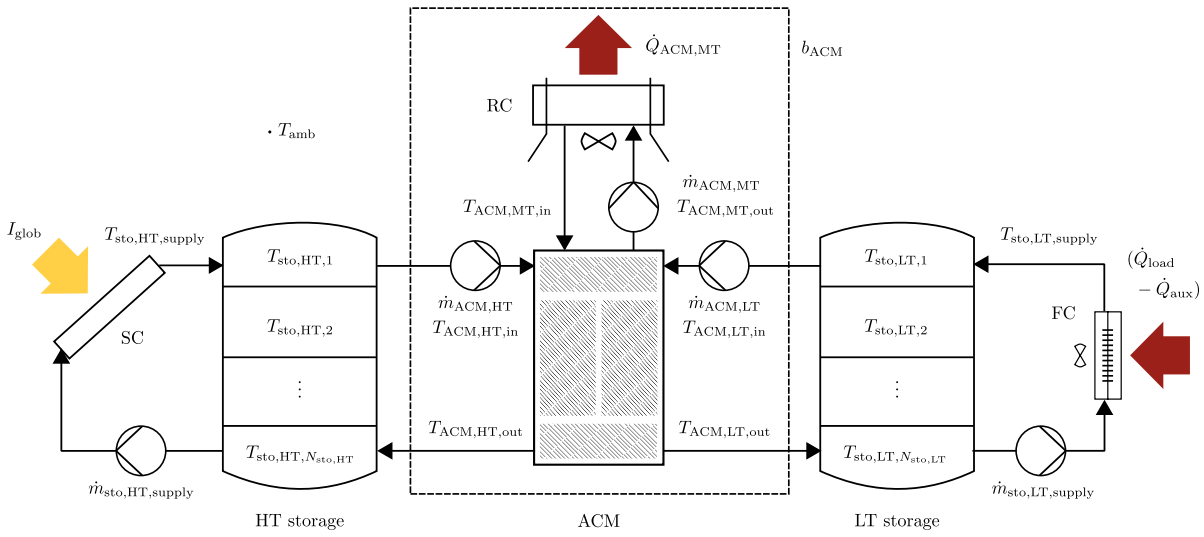

Figure 1. Schematic depiction of the solar thermal HVAC system considered within this study.

The system consists of solar collectors (SC) with total surface $A_{\mathrm{col}} = 31.35\,\mathrm{m}^2$ and optical efficiency $\eta_{\mathrm{col}} = 0.62$ that support a stratified high temperature water storage (HT storage) of volume $V_{\mathrm{sto,HT}} = 2.0\,\mathrm{m}^3$.[1] If the ACM is in operation, it uses the heated water from the top of the HT storage to absorb heat from a stratified low temperature water storage (LT storage) of volume $V_{\mathrm{sto,LT}} = 1.0\,\mathrm{m}^3$ and emits the combined heat through a recooling tower (RC).

The ACM operation conditions are determined by the current temperatures of the mass flows entering the machine. Favorable operation conditions are high values for the temperatures $T_{\mathrm{ACM,LT,in}}(t)$ and $T_{\mathrm{ACM,HT,in}}(t)$ and low values for the temperature $T_{\mathrm{ACM,MT,in}}(t)$ [1] with limits shown in Table 1. At optimal conditions, the ACM has a cooling capacity of $\dot{Q}_{\mathrm{ACM,LT,max}} = 12\,\mathrm{kW}$ and a Coefficient Of Performance (COP) of $\mathrm{COP}_{\mathrm{ACM,max}} = 0.65$.

[1] For simplicity, usual system separations of frost-proof outdoor circuits from indoor water circuits are neglected.

Table 1. Minimum and maximum ACM inlet temperatures for operation.

Inlet temperature	Minimum value	Maximum value
$T_{\mathrm{ACM,LT,in}}$	10 °C	22 °C
$T_{\mathrm{ACM,HT,in}}$	55 °C	95 °C
$T_{\mathrm{ACM,MT,in}}$	15 °C	40 °C

The water from the bottom of the LT storage can be used to compensate a heat load $\dot{Q}_{\mathrm{load}}$ arising from the cooling demand of a building through fan coils (FC). If the cooling capacity available from the LT storage is not sufficient to compensate $\dot{Q}_{\mathrm{load}}$, an auxiliary cooling device (e. g. a compression chiller) is used to generate $\dot{Q}_{\mathrm{aux}}$ which decreases the load of the system.

Further information on the parametrization and control strategies of the relevant system components is given in the following section.

3. Methodology

In the following, the chosen modeling approach for the system introduced in Section 2 is described, as well as the design and implementation of the considered conventional and optimization-based controllers.

3.1. Modeling approach

For system modeling, physically motivated gray-box models based on mass and energy balances are used. Since the model is to be later used within gradient-based optimization methods (see Section 3.3), it must fulfill all necessary conditions e. g. regarding differentiability, cf. [7].

For simplicity, all heat losses of components to their surroundings are neglected. The system is assumed to be filled with incompressible water with constant specific heat capacity $c_{\mathrm{W}} = 4.128\,\mathrm{kJ/(kgK)}$ and density $\rho_{\mathrm{W}} = 1\,\mathrm{kg/l}$. The different component models and their internal control strategies are explained in the following.

3.1.1. Modeling of the solar collector cycle For the solar collectors, a simplified model variant of [8] is chosen that converts the solar radiation $I_{\mathrm{glob}}(t)$ available at a time t to a heat flow $\dot{Q}_{\mathrm{col}}(t)$, according to the collector surface A_{col} and optical efficiency η_{col} as in

$$\dot{Q}_{\mathrm{col}}(t) = \eta_{\mathrm{col}} A_{\mathrm{col}} I_{\mathrm{glob}}(t). \tag{1}$$

Further, it is assumed that the collector-side pump is controlled in a way that the temperature of the medium that enters the top of the HT storage is constant with $T_{\mathrm{sto,HT,supply}} = 80\,^{\circ}\mathrm{C}$, and the mass flow $\dot{m}_{\mathrm{sto,HT,supply}}(t)$ is adjusted so that the medium extracted from the bottom of the HT storage $T_{\mathrm{sto,HT},N_{\mathrm{sto,HT}}}(t)$ can be heated up accordingly, i. e.,

$$\dot{m}_{\mathrm{sto,HT,supply}}(t) = \frac{\dot{Q}_{\mathrm{col}}(t)}{c_{\mathrm{W}}(T_{\mathrm{sto,HT,supply}} - T_{\mathrm{sto,HT},N_{\mathrm{sto,HT}}}(t))}. \tag{2}$$

3.1.2. Modeling of the load cycle On the load side, it is assumed that the temperature of the medium that enters the top of the LT storage is constant with $T_{\mathrm{sto,LT,supply}} = 20\,^{\circ}\mathrm{C}$, and the mass flow $\dot{m}_{\mathrm{sto,LT,supply}}(t)$ is adjusted to compensate for the heat flow of the load $\dot{Q}_{\mathrm{load}}(t)$ that

has not been covered by $\dot{Q}_{\mathrm{aux}}(t)$, according to the temperature of the bottom of the LT storage $T_{\mathrm{sto,LT},N_{\mathrm{sto,LT}}}(t)$, so that

$$\dot{m}_{\mathrm{sto,LT,supply}}(t) = \frac{\dot{Q}_{\mathrm{load}}(t) - \dot{Q}_{\mathrm{aux}}(t)}{c_{\mathrm{W}}(T_{\mathrm{sto,LT,supply}} - T_{\mathrm{sto,LT},N_{\mathrm{sto,LT}}}(t))}. \tag{3}$$

For this assumption to be applicable, it is ensured that the mass flow $\dot{m}_{\mathrm{sto,LT,supply}}(t)$ at all times is less than some maximum value $\dot{m}_{\mathrm{sto,LT,supply,max}}$, i. e.,

$$\dot{m}_{\mathrm{sto,LT,supply}}(t) \leq \dot{m}_{\mathrm{sto,LT,supply,max}}. \tag{4}$$

The auxiliary cooling device is only used to reduce the load for the system by $\dot{Q}_{\mathrm{aux}}(t)$ if $\dot{Q}_{\mathrm{load}}(t)$ at some time cannot be compensated from the LT storage alone.

3.1.3. Modeling of adsorption cooling machine and recooling system From the amount of heat exchanged by the machine's three circuits during an entire adsorption cycle [9] at certain operation conditions, energy balances can be formulated that allow to calculate the mean heat flows at a time during that cycle as in

$$\begin{aligned}
\dot{Q}_{\mathrm{ACM,LT}}(t) &= f_{\dot{Q}_{\mathrm{ACM,LT}}}(T_{\mathrm{ACM,HT,in}}(t), T_{\mathrm{ACM,MT,in}}(t), T_{\mathrm{ACM,LT,in}}(t)) \\
\dot{Q}_{\mathrm{ACM,HT}}(t) &= \frac{\dot{Q}_{\mathrm{ACM,LT}}(t)}{f_{\mathrm{COP}}(T_{\mathrm{ACM,HT,in}}(t), T_{\mathrm{ACM,MT,in}}(t), T_{\mathrm{ACM,LT,in}}(t))} \\
\dot{Q}_{\mathrm{ACM,MT}}(t) &= \dot{Q}_{\mathrm{ACM,LT}}(t) + \dot{Q}_{\mathrm{ACM,HT}}(t).
\end{aligned} \tag{5}$$

The functions $f_{\dot{Q}_{\mathrm{ACM,LT}}}(\cdot)$ and $f_{\mathrm{COP}}(\cdot)$ are fittings of quadratic polynomials to machine specific data for cooling power and COP at different operation conditions. Using the mass flows of the several circuits, here $\dot{m}_{\mathrm{ACM,LT}} = 48\,\mathrm{kg/min}$, $\dot{m}_{\mathrm{ACM,HT}} = 41.8\,\mathrm{kg/min}$ and $\dot{m}_{\mathrm{ACM,MT}} = 85.0\,\mathrm{kg/min}$, mean output temperatures can be obtained from

$$\begin{aligned}
T_{\mathrm{ACM,LT,out}}(t) &= T_{\mathrm{ACM,LT,in}}(t) - \frac{\dot{Q}_{\mathrm{ACM,LT}}(t)}{c_{\mathrm{W}}\dot{m}_{\mathrm{ACM,LT}}} \\
T_{\mathrm{ACM,HT,out}}(t) &= T_{\mathrm{ACM,HT,in}}(t) - \frac{\dot{Q}_{\mathrm{ACM,HT}}(t)}{c_{\mathrm{W}}\dot{m}_{\mathrm{ACM,HT}}} \\
T_{\mathrm{ACM,MT,out}}(t) &= T_{\mathrm{ACM,MT,in}}(t) + \frac{\dot{Q}_{\mathrm{ACM,MT}}(t)}{c_{\mathrm{W}}\dot{m}_{\mathrm{ACM,MT}}}.
\end{aligned} \tag{6}$$

Though the model is neglecting the cyclic behavior of an ACM as it is shown e. g. in [9], the model becomes applicable since the HT and LT storages connected to the ACM as well as the mass flow of the MT circuit are of sufficient size to dampen the effects of the fluctuating output temperatures. The model can be adapted to a specific machine without additional measurement devices apart from temperature and flow sensors, and depicts the functioning of the machine including it's internal control decisions.

Since the booting- and shutdown-phases of the ACM are not considered within this model, it must be ensured that the machine is switched on and off only with a reasonable frequency. Within this work, this is realized either through switching hystereses or minimum operation times.

The recooling system of the ACM is controlled to always provide cooling medium with temperature $T_{\mathrm{ACM,MT,in}}(t)$ that meets a constant temperature difference $\Delta T_{\mathrm{ACM,MT}}$ to the current ambient temperature $T_{\mathrm{amb}}(t)$, i. e.,

$$T_{\mathrm{ACM,MT,in}}(t) = T_{\mathrm{amb}}(t) + \Delta T_{\mathrm{ACM,MT}}. \tag{7}$$

3.1.4. Modeling of the storage tanks For modeling of the stratified storage tanks, their volumes are discretized into several layers for which an energy balance is calculated. Variants of this common approach can be found e. g. in [10, 11]. The model of the HT storage contains $N_{\mathrm{sto,HT}} = 4$ layers of mass $M_{\mathrm{sto,HT}}$ and the LT storage model $N_{\mathrm{sto,LT}} = 3$ layers of mass $M_{\mathrm{sto,LT}}$ according to

$$M_{\mathrm{sto,HT}} = \frac{\rho_{\mathrm{W}} V_{\mathrm{sto,HT}}}{N_{\mathrm{sto,HT}}},\ M_{\mathrm{sto,LT}} = \frac{\rho_{\mathrm{W}} V_{\mathrm{sto,LT}}}{N_{\mathrm{sto,LT}}}. \tag{8}$$

The temperature within a stratum is influenced by the amount and temperature of the mass flows entering and leaving it. The current existence of a possible mass flow is determined by the current status $b_{\mathrm{ACM}}(t)$ of the ACM, which is a binary variable that shows whether the machine is running ($b_{\mathrm{ACM}} = 1$) or not ($b_{\mathrm{ACM}} = 0$), and by the current values of $\dot{m}_{\mathrm{sto,HT,supply}}(t)$ and $\dot{m}_{\mathrm{sto,LT,supply}}(t)$.[2] The energy balance of the HT storage top layer with index 1 is shown in Eq. (9) and for the LT storage top layer with index 1 in Eq. (10), respectively:

$$\begin{aligned}\dot{T}_{\mathrm{sto,HT,1}}(t) = M_{\mathrm{sto,HT}}^{-1}[&\dot{m}_{\mathrm{sto,HT,supply}}(t) T_{\mathrm{sto,HT,supply}} \\ &- (1 - b_{\mathrm{ACM}}(t)) \dot{m}_{\mathrm{sto,HT,supply}}(t) T_{\mathrm{sto,HT,1}}(t) \\ &+ b_{\mathrm{ACM}}(t)(\dot{m}_{\mathrm{ACM,HT}} - \dot{m}_{\mathrm{sto,HT,supply}}(t)) T_{\mathrm{sto,HT,2}}(t) \\ &- b_{\mathrm{ACM}}(t) \dot{m}_{\mathrm{ACM,HT}} T_{\mathrm{sto,HT,1}}(t)],\end{aligned} \tag{9}$$

$$\begin{aligned}\dot{T}_{\mathrm{sto,LT,1}}(t) = M_{\mathrm{sto,LT}}^{-1}[&\dot{m}_{\mathrm{sto,LT,supply}}(t) T_{\mathrm{sto,LT,supply}} \\ &- (1 - b_{\mathrm{ACM}}(t)) \dot{m}_{\mathrm{sto,LT,supply}}(t) T_{\mathrm{sto,LT,1}}(t) \\ &+ b_{\mathrm{ACM}}(t)(\dot{m}_{\mathrm{ACM,LT}} - \dot{m}_{\mathrm{sto,LT,supply}}(t)) T_{\mathrm{sto,LT,2}}(t) \\ &- b_{\mathrm{ACM}}(t) \dot{m}_{\mathrm{ACM,LT}} T_{\mathrm{sto,LT,1}}(t)].\end{aligned} \tag{10}$$

The balance equations for the HT storage middle layers are shown in Eq. (11) and for the LT storage middle layers in Eq. (12):

$$\begin{aligned}\dot{T}_{\mathrm{sto,HT,k}}(t) = M_{\mathrm{sto,HT}}^{-1}[&(1 - b_{\mathrm{ACM}}(t)) \dot{m}_{\mathrm{sto,HT,supply}}(t) T_{\mathrm{sto,HT},k-1}(t) \\ &- b_{\mathrm{ACM}}(t)(\dot{m}_{\mathrm{ACM,HT}} - \dot{m}_{\mathrm{sto,HT,supply}}(t)) T_{\mathrm{sto,HT},k}(t) \\ &+ b_{\mathrm{ACM}}(t)(\dot{m}_{\mathrm{ACM,HT}} - \dot{m}_{\mathrm{sto,HT,supply}}(t)) T_{\mathrm{sto,HT},k+1}(t) \\ &- (1 - b_{\mathrm{ACM}}(t)) \dot{m}_{\mathrm{sto,HT,supply}}(t) T_{\mathrm{sto,HT},k}(t)], \qquad k = 2, \ldots, N_{\mathrm{sto,HT}} - 1,\end{aligned} \tag{11}$$

$$\begin{aligned}\dot{T}_{\mathrm{sto,LT,k}}(t) = M_{\mathrm{sto,LT}}^{-1}[&(1 - b_{\mathrm{ACM}}(t)) \dot{m}_{\mathrm{sto,LT,supply}}(t) T_{\mathrm{sto,LT},l-1}(t) \\ &- b_{\mathrm{ACM}}(t)(\dot{m}_{\mathrm{ACM,LT}} - \dot{m}_{\mathrm{sto,LT,supply}}(t)) T_{\mathrm{sto,LT},l}(t) \\ &+ b_{\mathrm{ACM}}(t)(\dot{m}_{\mathrm{ACM,LT}} - \dot{m}_{\mathrm{sto,LT,supply}}(t)) T_{\mathrm{sto,LT},l+1}(t) \\ &- (1 - b_{\mathrm{ACM}}(t)) \dot{m}_{\mathrm{sto,LT,supply}}(t) T_{\mathrm{sto,LT},l}(t)], \qquad l = 2, \ldots, N_{\mathrm{sto,LT}} - 1.\end{aligned} \tag{12}$$

The energy balance for the HT storage bottom layer with index $N_{\mathrm{sto,HT}}$ is shown in Eq. (13) and for the LT storage bottom layer with index $N_{\mathrm{sto,LT}}$ in Eq. (14):

[2] For the system considered here, it can be assumed that $\dot{m}_{\mathrm{ACM,HT}}(t) \geq b_{\mathrm{ACM}}(t) \dot{m}_{\mathrm{sto,HT,supply}}(t)$ and $\dot{m}_{\mathrm{ACM,LT}}(t) \geq b_{\mathrm{ACM}}(t) \dot{m}_{\mathrm{sto,LT,supply}}(t)$ at all times. If this is not the case, further expressions that take into account the additional mass flow directions need to be added to the models.

$$\begin{aligned}\dot{T}_{\mathrm{sto,HT,N_{sto,HT}}}(t) = M^{-1}_{\mathrm{sto,HT}}[&(1-b_{\mathrm{ACM}}(t))\dot{m}_{\mathrm{sto,HT,supply}}(t)T_{\mathrm{sto,HT,N_{sto,HT}-1}}(t)\\ &-\dot{m}_{\mathrm{sto,HT,supply}}(t)T_{\mathrm{sto,HT,N_{sto,HT}}}(t)\\ &+b_{\mathrm{ACM}}(t)\dot{m}_{\mathrm{ACM,HT}}T_{\mathrm{ACM,HT,OUT}}(t)\\ &-b_{\mathrm{ACM}}(t)(\dot{m}_{\mathrm{ACM,HT}}-\dot{m}_{\mathrm{sto,HT,supply}}(t))T_{\mathrm{sto,HT,N_{sto,HT}}}(t)],\end{aligned} \tag{13}$$

$$\begin{aligned}\dot{T}_{\mathrm{sto,LT,N_{sto,LT}}}(t) = M^{-1}_{\mathrm{sto,LT}}[&(1-b_{\mathrm{ACM}}(t))\dot{m}_{\mathrm{sto,LT,supply}}(t)T_{\mathrm{sto,LT,N_{sto,LT}-1}}(t)\\ &-\dot{m}_{\mathrm{sto,LT,supply}}(t)T_{\mathrm{sto,LT,N_{sto,LT}}}(t)\\ &+b_{\mathrm{ACM}}(t)\dot{m}_{\mathrm{ACM,LT}}T_{\mathrm{ACM,LT,OUT}}(t)\\ &-b_{\mathrm{ACM}}(t)(\dot{m}_{\mathrm{ACM,LT}}-\dot{m}_{\mathrm{sto,LT,supply}}(t))T_{\mathrm{sto,LT,N_{sto,LT}}}(t)].\end{aligned} \tag{14}$$

3.2. Formulation of a conventional control scheme

To simulate a conventional, set-point based control scheme, the model introduced in Section 3.1 is used within a system simulation in OpenModelica [12]. The ACM operation status $b_{\mathrm{ACM}}(t)$ is determined using the control scheme

$$b_{\mathrm{ACM}}(t) = \begin{cases} 1, & \text{if } T_{\mathrm{sto,HT,1}}(t) \geq 60\,^{\circ}\mathrm{C} \wedge T_{\mathrm{sto,LT,N_{sto,LT}}}(t) \geq 12\,^{\circ}\mathrm{C},\\ 0, & \text{if } T_{\mathrm{sto,HT,1}}(t) < 55\,^{\circ}\mathrm{C} \vee T_{\mathrm{sto,LT,N_{sto,LT}}}(t) < 10\,^{\circ}\mathrm{C}.\end{cases} \tag{15}$$

If $T_{\mathrm{sto,HT,1}}$ is sufficient for operating the ACM, and $T_{\mathrm{sto,LT,N_{sto,LT}}}$ is not too low, the ACM is switched on. If either $T_{\mathrm{sto,HT,1}}$ or $T_{\mathrm{sto,LT,N_{sto,LT}}}$ are too low, the ACM is switched off. A hysteresis is introduced for both temperature constraints to avoid frequent switching (or in simulation, chattering). Predictions for driving energy and load are not considered.

3.3. Formulation of an optimization-based scheduling method

The aim of the optimization-based control approach is to run the system in a way that minimizes the total use of auxiliary cooling over the considered period, taking into account system dynamics and operation conditions and boundaries as well as cooling demand, solar radiation and ambient temperature profiles. This results in the Mixed-Integer Nonlinear Optimal Control Problem (MINOCP)

$$\underset{x(\cdot),b_{\mathrm{ACM}}(\cdot)}{\text{minimize}} \quad \int_{t_0}^{t_\mathrm{f}} \dot{Q}_{\mathrm{aux}}(t)\,\mathrm{d}t \tag{16a}$$

$$\text{subject to} \quad (1)\text{-}(14) \tag{16b}$$

$$x(t) = \begin{pmatrix} T_{\mathrm{sto,HT},k}(t),\ k=1,\ldots,N_{\mathrm{sto,HT}} \\ T_{\mathrm{sto,LT},l}(t),\ l=1,\ldots,N_{\mathrm{sto,LT}} \end{pmatrix},\ u(t) = \begin{pmatrix} T_{\mathrm{amb}}(t) \\ \dot{Q}_{\mathrm{Load}}(t) \\ I_{\mathrm{glob}}(t) \end{pmatrix} \tag{16c}$$

$$T_{\mathrm{ACM,LT,IN}}(t) + M_{\mathrm{ACM,LT,IN,min}}(1-b_{\mathrm{ACM}}(t)) \geq T_{\mathrm{ACM,LT,IN,min}} \tag{16d}$$

$$T_{\mathrm{ACM,HT,IN}}(t) + M_{\mathrm{ACM,HT,IN,min}}(1-b_{\mathrm{ACM}}(t)) \geq T_{\mathrm{ACM,HT,IN,min}} \tag{16e}$$

$$b_{\mathrm{ACM}}(t) \in \{0,1\}, \quad t \in [t_0, t_\mathrm{f}] \tag{16f}$$

$$x_{\min} \leq x(t) \leq x_{\max}, \quad t \in [t_0, t_\mathrm{f}] \tag{16g}$$

$$x(0) = x_0. \tag{16h}$$

The aim of minimizing the total auxiliary cooling is stated in the objective in Eq. (16a), the system dynamics are considered in Eq. (16b) for all states x and profiles u in Eq. (16c). The linear inequalities in Eq. (16d) and (16e) ensure that the ACM is operated only within valid

conditions, see e. g. [13].[3] In Eq. (16f) it is assured that the ACM can only be switched on or off. Maximum and minimum system temperatures are specified in Eq. (16g) to prevent the water from freezing or boiling. Finally in Eq. (16h), it is ensured that the initial values of x match the initial state values of the simulation.

For solving, the MINOCP in Eq. (16) is transformed into a Mixed-Integer Non-Linear Program (MINLP) using direct collocation [7] with Lagrange polynomials on an equidistant time grid of step size $\Delta t = 120\,\mathrm{s}$ using the symbolic optimization framework CasADi [14, 15]. Power-cycling the ACM is made possible only every 1800 s to keep the amount of integer variables of the MINLP reasonable, as well as to incorporate the minimum operation time of the ACM (cf. Section 3.1). The MINLP is solved from CasADi using the MINLP solver BONMIN [16] that incorporates IPOPT [17] as NLP solver, which here uses MA57 [18] as linear solver.

4. Results and discussion

A comparison of the controller performances is carried out for a typical scenario of energy availability and load appearance where the load appears delayed from the main availability of the solar irradiation, for a time horizon of 24 hours. The load is calculated from the current ambient temperature $T_{\mathrm{amb}}(t)$ and the target building temperature $T_{\mathrm{target}} = 22\,^{\circ}\mathrm{C}$ as

$$\dot{Q}_{\mathrm{load}}(t) = \begin{cases} 0.0\,\mathrm{kW}, & \text{if } T_{\mathrm{amb}}(t) \leq T_{\mathrm{target}}, \\ 0.9\,\frac{\mathrm{kW}}{\mathrm{K}}(T_{\mathrm{amb}}(t) - T_{\mathrm{target}}), & \text{if } T_{\mathrm{amb}}(t) > T_{\mathrm{target}}. \end{cases} \tag{17}$$

4.1. Application of the conventional controller

A depiction of the simulation results for the conventional controller, computed in less than 1 s on an Intel Core i5-4570 3.20 GHz CPU, is shown in Figure 2. It can be seen that the ACM is switched on relatively early in the day and working with high values for $\dot{Q}_{\mathrm{ACM,LT}}$ and COP due to the low values of T_{amb} that facilitate low values for $T_{\mathrm{ACM,MT,in}}$. However, this is merely coincidental, since the controller does not actively consider T_{amb}. During that time, the ACM is power-cycled several times, since the driving energy supplied by the collectors to the HT storage is not yet sufficient for permanent operation. Since no load occurs before 10:00, the operation of the ACM causes low LT storage temperatures, and with this, inefficient operation conditions.

The occurring load cannot be compensated completely by the system alone, and auxiliary cooling power becomes necessary.[4] It is shown that the ACM is running with a cooling power lower than the occurring load for a long time. One reason for this is that the driving energy from the early day has already been utilized, often within inefficient operation conditions.

These results reveal a systematic problem, since this situation is likely to happen if the load occurs later than the availability of the driving energy, and the controller is neither aware of the time when the load occurs nor of the amount of driving energy available throughout the day. Changing the temperature boundaries for switching the ACM cannot finally eliminate this problem, since the specific occurrence of the problem is dependent on the daily load and driving energy situation. However, this problem can be countered by applying predictive, optimization-based control strategies, as shown in the next section.

4.2. Application of the optimization-based controller

The solution of the MINLP for the optimization-based controller, which takes about 415 s on an Intel Core i5-4570 3.20 GHz CPU, is depicted in Figure 3, where multiple aspects show that the

[3] Only these operation limits have to be actively considered within this study. Other limits for ACM operation as shown in Table 1 cannot be reached due to the problem setup.

[4] In case such an auxiliary cooling device would not be available, insufficient cooling power would result in the building temperature to rise above the target temperature.

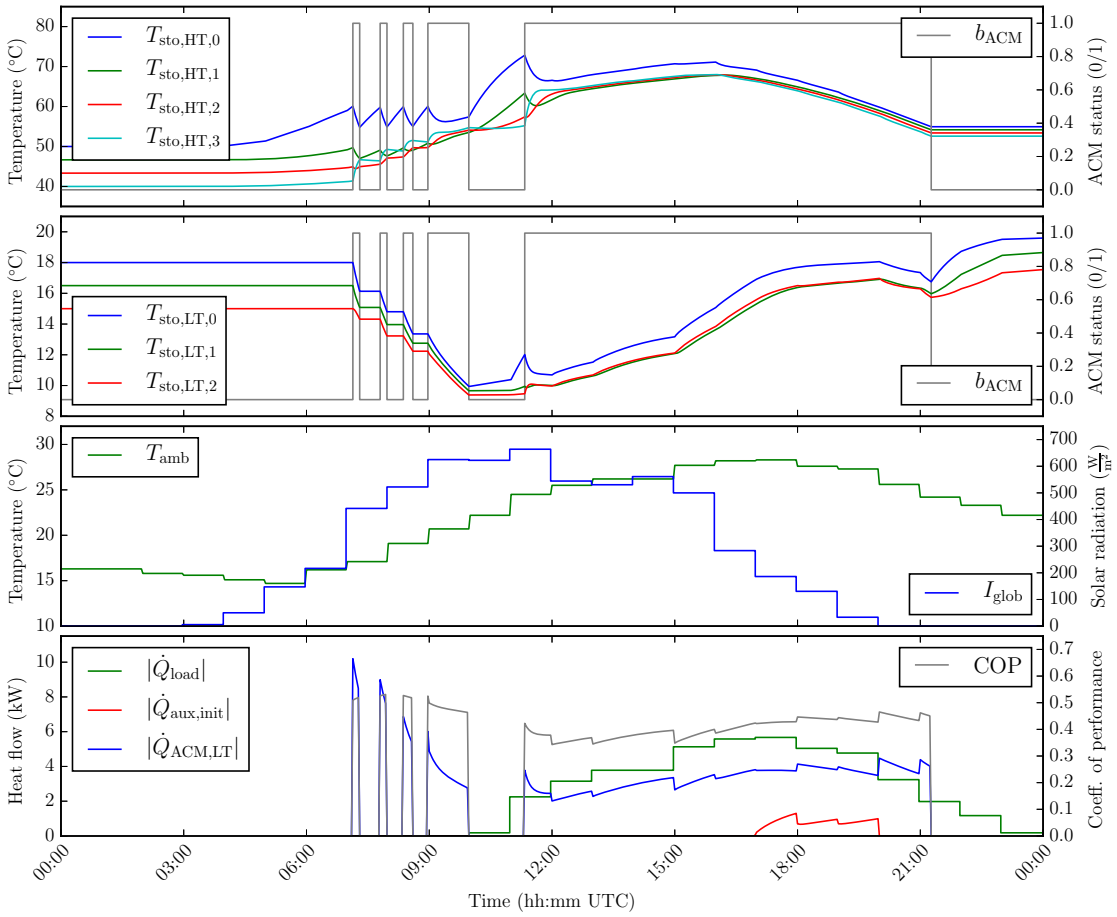

Figure 2. Simulation results using the control scheme in Eq. (15).

controller actively aims towards running the ACM more efficiently.

In the early day, it first increases the HT storage temperature more than the conventional controller, but still operates the ACM for some period before load occurrence to profit from the still comparatively low ambient temperatures. Afterwards, it heats up the HT storage, and also heats up the LT storage to compensate the now occurring load, which again creates favorable ACM operation conditions. Then, it runs the ACM for a longer period with comparatively high LT storage temperatures to again favor efficiency. At the end of the day, it runs the ACM one more time to profit once more from lower ambient temperatures to compensate for the final cooling demands of the day. At all times, the ACM is operated only within valid conditions. In that way, the auxiliary cooling demand has been reduced widely, as shown in the next section.

4.3. Comparison of controller performances

A comparison of the controller performances is given by a comparison of the integrated auxiliary cooling power as well as the integrated ACM operation time for the conventional and optimization-based control strategy in Figure 4.

In comparison to the conventional control strategy, the total demand for auxiliary cooling is reduced for this example by approximately a quarter using the optimization-based control strategy. This is a direct result of the objective formulation in Eq. (16a), and is obtained via a more efficient operation of the ACM.

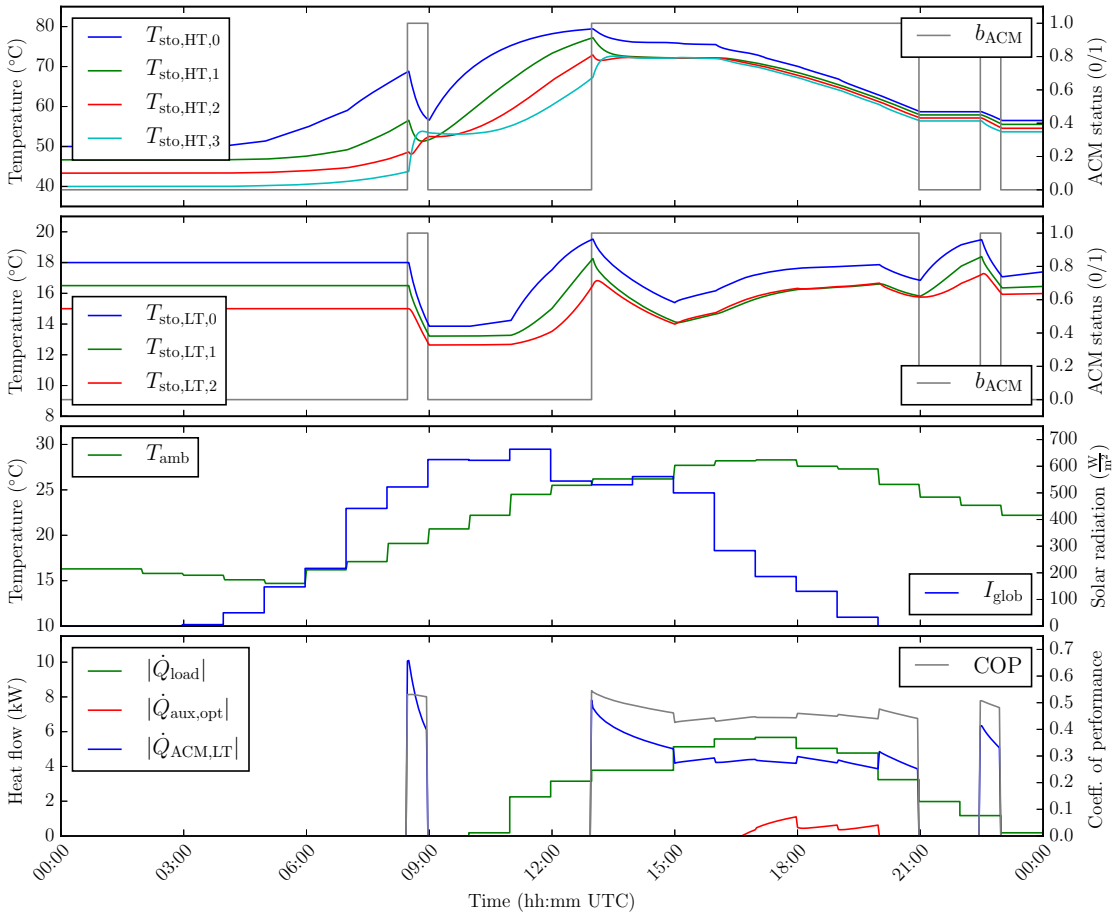

Figure 3. Solution of the MINLP arising from the MINOCP in Eq. (16).

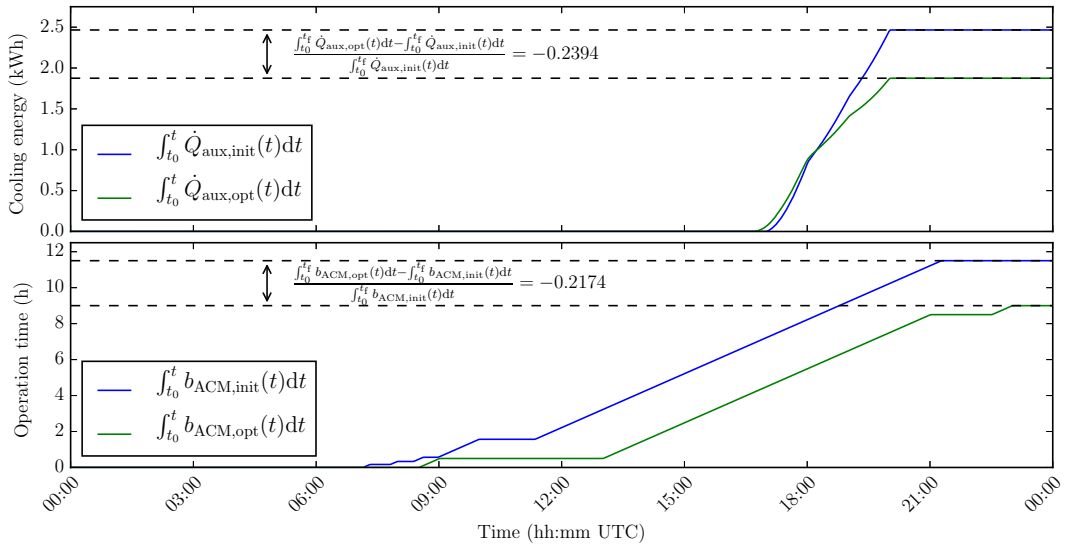

Figure 4. Comparison of controller performances.

Implicitly, a more efficient operation of the ACM, and with this, a more efficient use of the available driving energy, results in a shorter integrated operation time of the ACM. Thus, in addition to the reduced auxiliary cooling demand, the total ACM runtime is reduced by more than 20 % using the optimization-based control strategy, saving electricity cost for ACM, pump and especially recooling tower operation.

5. Conclusions and future work

Within this work, advantages of using predictive control methods for operation scheduling of a silica-gel/water ACM have been exemplified on a simulation study. Using the optimization-based control approach, the use of auxiliary cooling power supply could be reduced, which simultaneously resulted in a reduction of the total operation time of the ACM.

The examinations should now be carried out for other scenarios of driving energy and load occurrence. Due to its predictive nature, it can be expected that the optimization-based approach is well suited also for scenarios of fluctuating availability of driving energy.

For practical application of this approach for system control, an extended, closed-loop model-predictive control approach should be implemented, i. e., the MINLP should be solved repeatedly during operation of the system based on the current system state to compensate for model mismatches, prediction errors and other operation disturbances. This creates need for an optimization routine that can solve the problem almost in real-time and requires further investigation.

Acknowledgments

Support by the EU via ITN-TEMPO (607957) and ITN-AWESCO (642 682), by DFG via Research Unit FOR 2401, by BMWi via the project eco4wind and by Ministerium fuer Wissenschaft, Forschung und Kunst Baden-Wuerttemberg (Az: 22-7533.-30-20/9/3) is gratefully acknowledged.

References

[1] Chang W S, Wang C C and Shieh C C 2007 *Applied Thermal Engineering* **27** 2195 – 2199 ISSN 1359-4311
[2] Gräber M 2013 *Energieoptimale Regelung von Kälteprozessen* Ph.D. thesis
[3] Bau U, Braatz A L, Lanzerath F, Herty M and Bardow A 2015 *International Journal of Refrigeration* **56** 52 – 64 ISSN 0140-7007
[4] Nienborg B, Dalibard A, Schnabel L and Eicker U 2017 *Applied Energy* **185, Part 1** 732 – 744 ISSN 0306-2619
[5] Choudhury B, Saha B B, Chatterjee P K and Sarkar J P 2013 *Applied Energy* **104** 554 – 567 ISSN 0306-2619
[6] Afram A and Janabi-Sharifi F 2014 *Building and Environment* **72** 343 – 355 ISSN 0360-1323
[7] Biegler L 2010 *Nonlinear Programming* (Society for Industrial and Applied Mathematics)
[8] Ferhatbegovic T, Zucker G and Palensky P 2011 *Proceedings of 10th IEEE AFRICON*
[9] Núñez T 2010 *Journal of Sustainable Energy* **10**
[10] Streckiene G, Martinaitis V and Vaitiekunas P 2011 *8th International Conference on Environmental Engineering*
[11] Ferhatbegovic T, Palensky P, Fontanella G and Basciotti D 2012 *21st IEEE International Symposium on Industrial Electronics - ISIE2012*
[12] The Open Source Modelica Consortium 2017 OpenModelica URL `https://www.openmodelica.org`
[13] Glover F 1975 *Management Science* **22**
[14] Andersson J 2013 *A General-Purpose Software Framework for Dynamic Optimization* Ph.D. thesis Department of Electrical Engineering (ESAT/SCD) and Optimization in Engineering Center, KU Leuven
[15] Andersson J, Gillis J and Diehl M 2017 *User Documentation for CasADi* URL `http://casadi.sourceforge.net/users_guide/casadi-users_guide.pdf`
[16] Bonami P, Biegler L T, Conn A R, Cornuéjols G, Grossmann I E, Laird C D, Lee J, Lodi A, Margot F, Sawaya N and Wächter A 2008 *Discrete Optimization* **5** 186 – 204 ISSN 1572-5286
[17] Wächter A and Biegler L T 2006 *Mathematical Programming* **106** 25–57 ISSN 1436-4646
[18] HSL 2017 A collection of fortran codes for large scale scientific computation URL `http://www.hsl.rl.ac.uk/`